Proceedings of the
International Conference on Mechanical Engineering and Renewable Energy 2011
(ICMERE2011) 22- 24 December 2011, Chittagong, Bangladesh

ICMERE2011-PI-127

ENTRY FLOW SUBJECTED TO HIGH REYNOLDS NUMBER

M. A. Masud[*], **Prabir Kumar Bhattacharjee**[1] **and Md. Mahmud Alam**[2]

[*] Institute of Natural Science, United International University, Dhanmondi, Dhaka, Bangladesh
[1] Mathematics Department, Govt. Rajendra College, Faridpur, Bangladesh
[2] Mathematics Discipline, Khulna University, Khulna, Bangladesh
masud_math@ymail.com[*], alam_mahmud2000@yahoo.com[2]

Abstract*- Laminar entry flow through a curved pipe of circular cross-section has been considered. Variable Pressure gradient force is experienced at every cross-section. To study the flow phenomena at every cross-section, three dimensional momentum equations and the continuity equation have been considered in toroidal coordinate system. The problem has been solved numerically using SIMPLE algorithm. The Renolds number is found as one of the important flow governing parameters. In the present study, higher Reynolds number 1100 and 900 is considered.*

Keywords: Entry flow, Curved pipe, Reynolds Number.

1. INTRODUCTION

Flow through pipes or ducts are useful in different engineering phenomena. The application of curved pipe is found in equipments for example: heat exchangers, separators, piping systems, etc.

When the flow enters into the pipe, the velocities of all the particles are same. As the flow enters, the particles experience friction with the wall. This was studied by Sinha and Aggarwal[1]. They studied flow development from the entry to the fully developed region. They followed Van Dyke's approach of matched asymptotic expansions [2] and analyzed the problem considering uniform flow at the entry. The development of the flow is studied by considering three regions: (1) an inviscid core, (2) the boundary layer and (3) the down stream region. The boundary layer was found to grow until it becomes equal to the radius of the pipe. Also the velocity increases more rapidly during the initial development in comparison to the flow in the downstream region.

To study entry flow in a pipe Briley [3] used alternating direction implicit method to integrate the momentum equation without streamwise diffusion terms. Morihar and Cheng [4] presented a finite-difference solution of the complete Navier-Stokes equations, for entry flow in a two dimensional channel. They used Stokes flow(Re=0) as initial solution of the Navier-Stokes equations, then generated the solution for larger Reynolds number by iterating on the quasi-linearized Navier-stokes equations.

In case of curved pipe, the particles experience centrifugal force in addition to frictional force. Singh [5] obtained a solution of developing flow in a curved circular pipe by applying perturbation technique, where boundary layer method was assumed for the flow to be consisted of an inviscid core surrounded by secondary flow boundary layer. As the flow rate increases the secondary flow layer becomes thinner near the outer bend and thicker near the inner bend. The boundary layer near the inner bend eventually separate and interacts with the inviscid core.

Later Singh et al [6] extended this problem to a matter of more physiological importance. Here they considered an entrance profile of the form $w = \dfrac{Q(t)}{1 + \delta \cos \alpha}$, which is the case of blood being pumped from the left ventricle into the ascending aorta. A boundary-layer analysis is applied to determine the effects of curvature and an adverse pressure gradient on the wall shear. They showed the development of negative wall shear and backflow near the wall during the decelerating phase of the cycle as the boundary layer grows. The analysis also reveals how the increasing effect of the secondary flow draws off slower moving fluid azimuthally from the outer bend to the inner bend; this induces a cross-flow of faster moving fluid from the inner bend to the outer bend which results in a thinning of the boundary layer at the outer bend and a thickening at the inner bend. This implies an increased wall shear at the outer bend compared with that at the inner bend as the flow develops further downstream; this is in contrast with the initial stages of the motion near the entrance where the higher wall shear occurs at the inner bend owing to the external flow and to geometric factors. The analysis shows that the displacement effect of the boundary layer on the core is not significant because the boundary layer remains thin, about one-tenth of the tube diameter.

Soh and Berger[7] solved elliptic Navier-Stokes equation for entrance flow into a curved pipe using the artificial compressibility technique. Calculations were

carried out for curvature ratios $\frac{1}{7}$, $\frac{1}{20}$ and for Dean number 108.2 to 680.3. Secondary flow separation was observed near the inner wall in the developing region of the curved pipe. The separation and the magnitude of the secondary flow are found to be extremely influenced by curvature ratio.

Recently Masud and Alam [8] studied the effect of curvature ratio on the entry flow. But that was for low Reynolds number. In this paper our area of interest is the flow in the entry region under high Reynolds number.

2. MATHEMATICAL MODEL

The physical construction of the problem has been shown in Fig. 1. The toroidal coordinate system (r', θ, s') considered for the present study. The radius of the pipe is R and the radius of the uniform cross-section is a, the velocity components along r', θ, s' directions are u', v', w' respectively, p' is the pressure, ρ is the constant density of the fluid and υ is the kinematic viscosity of the fluid.
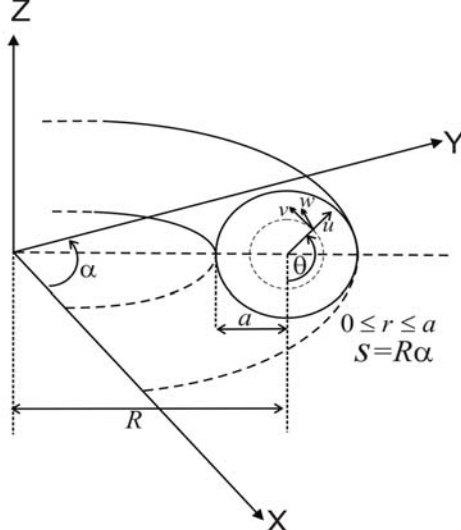

Fig. 1: Toroidal coordinate system for a curved pipe with circular cross-section

Introducing the non-dimensional variables, $u = \dfrac{u'}{W_\circ}, v = \dfrac{v'}{W_\circ}, w = \dfrac{w'}{W_\circ}, p = \dfrac{p'}{\rho W_\circ^2}, r = \dfrac{r'}{a}$ we get the following flow governing equations.

Non-dimensional continuity equation:

$$\frac{\partial}{\partial r}(r\omega u) + \frac{\partial}{\partial \theta}(\omega v) + \frac{\partial}{\partial s}(rw) = 0$$

Non-dimensional radial momentum equation:

$$\frac{1}{r\omega}\left[\frac{\partial}{\partial s}(ruw) + \frac{\partial}{\partial r}(r\omega u^2) + \frac{\partial}{\partial \theta}(\omega uv) - \omega v^2\right.$$
$$-\delta rw^2 \sin\theta\Big] = -\frac{\partial p}{\partial r} + \frac{1}{R_e}\left[\frac{1}{r\omega}\left\{\frac{\partial}{\partial r}\left(r\omega\frac{\partial u}{\partial r}\right)\right.\right.$$
$$+\frac{\partial}{\partial \theta}\left(\frac{\omega}{r}\frac{\partial u}{\partial \theta}\right) + \frac{\partial}{\partial s}\left(\frac{r}{\omega}\frac{\partial u}{\partial s}\right)\right\} - \frac{1}{r^2}\left(2\frac{\partial v}{\partial \theta} + u\right)$$
$$-\frac{v\delta}{\omega r}\cos\theta - \frac{\delta^2}{\omega^2}\left(\frac{2}{\delta}\frac{\partial w}{\partial s} + u\sin\theta + v\cos\theta\right)\sin\theta\Big]$$

Non-dimensional circumferential momentum equation:

$$\frac{1}{r\omega}\left[\frac{\partial}{\partial s}(rvw) + \frac{\partial}{\partial r}(ruv\omega) + \frac{\partial}{\partial \theta}(\omega v^2) + \omega uv\right.$$
$$-\delta rw^2 \cos\theta\Big] = -\frac{1}{r}\frac{\partial p}{\partial \theta} + \frac{1}{R_e}\left[\frac{1}{r\omega}\left\{\frac{\partial}{\partial r}\left(r\omega\frac{\partial v}{\partial r}\right)\right.\right.$$
$$+\frac{\partial}{\partial \theta}\left(\frac{\omega}{r}\frac{\partial v}{\partial \theta}\right) + \frac{\partial}{\partial s}\left(\frac{r}{\omega}\frac{\partial v}{\partial s}\right)\right\} + \frac{1}{r^2}\left(2\frac{\partial u}{\partial \theta} - v\right) +$$
$$\frac{u\delta}{\omega r}\cos\theta - \frac{\delta^2}{\omega^2}\left(\frac{2}{\delta}\frac{\partial w}{\partial s} + u\sin\theta + v\cos\theta\right)\cos\theta\Big]$$

Non-dimensional axial momentum equation:

$$\frac{1}{r\omega}\left[\frac{\partial}{\partial s}(rw^2) + \frac{\partial}{\partial r}(r\omega uw) + \frac{\partial}{\partial \theta}(\omega vw)\right.$$
$$+rw\delta(u\sin\theta + v\cos\theta)\Big] = -\frac{1}{\omega}\frac{\partial p}{\partial s}$$
$$+\frac{1}{R_e}\left[\frac{1}{r\omega}\left\{\frac{\partial}{\partial r}\left(r\omega\frac{\partial w}{\partial r}\right) + \frac{\partial}{\partial \theta}\left(\frac{\omega}{r}\frac{\partial w}{\partial \theta}\right) + \frac{\partial}{\partial s}\left(\frac{r}{\omega}\frac{\partial w}{\partial s}\right)\right\}\right.$$
$$+\frac{2\delta^2}{\omega^2}\left(\frac{\sin\theta}{\delta}\frac{\partial u}{\partial s} - \frac{\cos\theta}{\delta}\frac{\partial v}{\partial s} - \frac{w}{2}\right)\Big]$$

where, $R_e = \dfrac{aW_\circ}{\upsilon}$, $\omega = 1 + r\delta\sin\theta$ and $\delta = \dfrac{a}{R}$.

3. BOUNDARY CONDITIONS

The fluid flow boundary is considered to be consisted of three regions: the inlet cross-section, the rigid wall and the cross-section far downstream where the flow is assumed to be fully developed.

The initial conditions at the inlet is considered as,

$$w(r,\theta,0) = \frac{1}{1+\delta r\sin\theta} \quad , \quad u(r,\theta,0) = v(r,\theta,0) = 0$$

and $p = -\dfrac{1}{2(1+\delta r\sin\theta)^2}$.

Due to the no-slip condition, all the velocity components vanish at the rigid boundary, i.e., $u(1,\theta,s) = v(1,\theta,s) = w(1,\theta,s) = 0$.

At far down stream when the flow gets fully developed,
$\dfrac{\partial u}{\partial s} = \dfrac{\partial v}{\partial s} = \dfrac{\partial w}{\partial s} = 0$.

4. FINITE DIFFERENCE FORMULATIONS

To rewrite the momentum equations (1-3) and 4 into a practical finite-difference scheme of computation , the grid arrangement shown in Fig. 2 and Fig. 3 has been chosen.
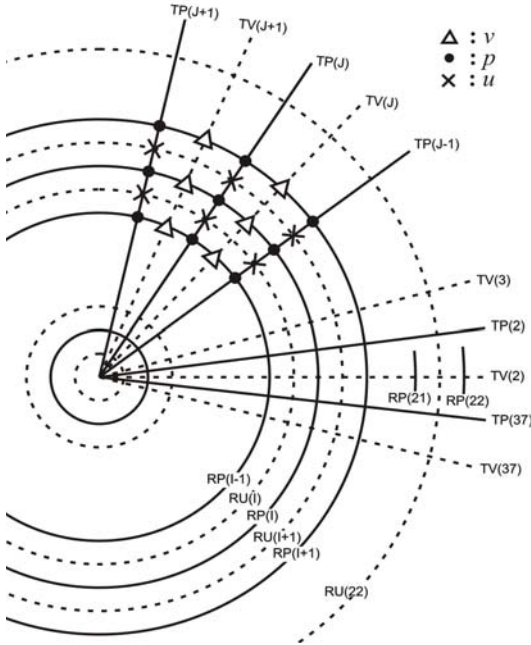

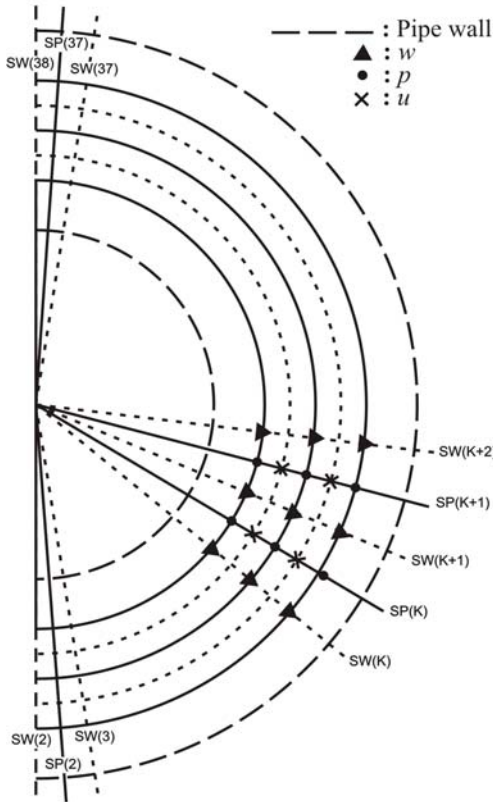Fig. 2: Grid system in the cross-section.

Fig. 3: Grid system in the horizontal plane passing through the axis of the pipe.

In radial direction 20 intermediate grid points have

been considered and in circumferential and axial direction 36 intermediate grid points have been considered. The grid has been arranged in such a way that pressure is defined at the centre of a cell and u, v, w are defined at different positions on the pressure cell boundaries. Then the momentum equations in u, v, w -directions reduces to,

$$a_{ijk}^u u_{ijk} = a_{i+1\,jk}^u u_{i+1\,jk} + a_{i-1\,jk}^u u_{i-1\,jk} + a_{ij+1k}^u u_{ij+1k}$$
$$+ a_{ij-1k}^u u_{ij-1k} + a_{ijk+1}^u u_{ijk+1} + a_{ijk-1}^u u_{ijk-1}$$
$$+ b^u + A_{ijk}^u \left(p_{i-1\,jk} - p_{ijk} \right)$$

$$a_{ijk}^v v_{ijk} = a_{i+1\,jk}^v v_{i+1\,jk} + a_{i-1\,jk}^v v_{i-1\,jk} + a_{ij+1k}^v v_{ij+1k}$$
$$+ a_{ij-1k}^v v_{ij-1k} + a_{ijk+1}^v v_{ijk+1} + a_{ijk-1}^v v_{ijk-1}$$
$$+ b^v + A_{ijk}^v \left(p_{ij-1k} - p_{ijk} \right)$$

$$a_{ijk}^w w_{ijk} = a_{i+1\,jk}^w w_{i+1\,jk} + a_{i-1\,jk}^w w_{i-1\,jk} + a_{ij+1k}^w w_{ij+1k}$$
$$+ a_{ij-1k}^w w_{ij-1k} + a_{ijk+1}^w w_{ijk+1} + a_{ijk-1}^w w_{ijk-1}$$
$$+ b^w + A_{ijk}^w \left(p_{ijk-1} - p_{ijk} \right)$$

respectively. And the continuity equation reduces to,

$$a_p p_p' = a_E p_E' + a_W p_W' + a_N p_N' + a_S p_S' + a_T p_T'$$
$$+ a_B p_B' + b$$

The accuracy is assured by taking $DIF < 10^{-6}$, where

$$DIF = \sum\sum\sum \begin{matrix} \{u_{n+1}(i,j,k) - u_n(i,j,k)\}^2 + \\ \{v_{n+1}(i,j,k) - v_n(i,j,k)\}^2 + \\ \{w_{n+1}(i,j,k) - w_n(i,j,k)\}^2 \end{matrix}$$

6. RESULTS AND DISCUSSION

Calculations have been carried out for Reynolds Number Re= 900 and 1100 at curvature $\delta = 0.1$ to understand the effect of high Reynolds number on flow in the entry region of a curved pipe. The problem has been solved using finite difference technique.

The results have been shown through vector plots of the secondary flow and contour plots of the axial flow. Also the axial velocity profile on the plane of symmetry has been shown by line chart. In all these cases, inner side is to the left and outer side is to the right. The arrows in the vector plots denote the direction and magnitude of the secondary velocity. In case of contour plots the distance between two consecutive contours is adjusted automatically and kept invariant.

6.1 Secondary flow development

The vector plots of the secondary flow have been shown in Fig. 4 for Reynolds number 900 and 1100 respectively. Two vortex secondary flow has been found which is symmetric about the horizontal line passing through the centre of cross-section. The secondary flow is set up just after entering the inlet due to the effect of centrifugal force. Circumferential velocity is greater for the particles near the upper and lower boundary. Also the velocity of the particles at the centre of cross-section is radially outward for the effect of centrifugal force. As the flow goes downstream the secondary velocity of the particles
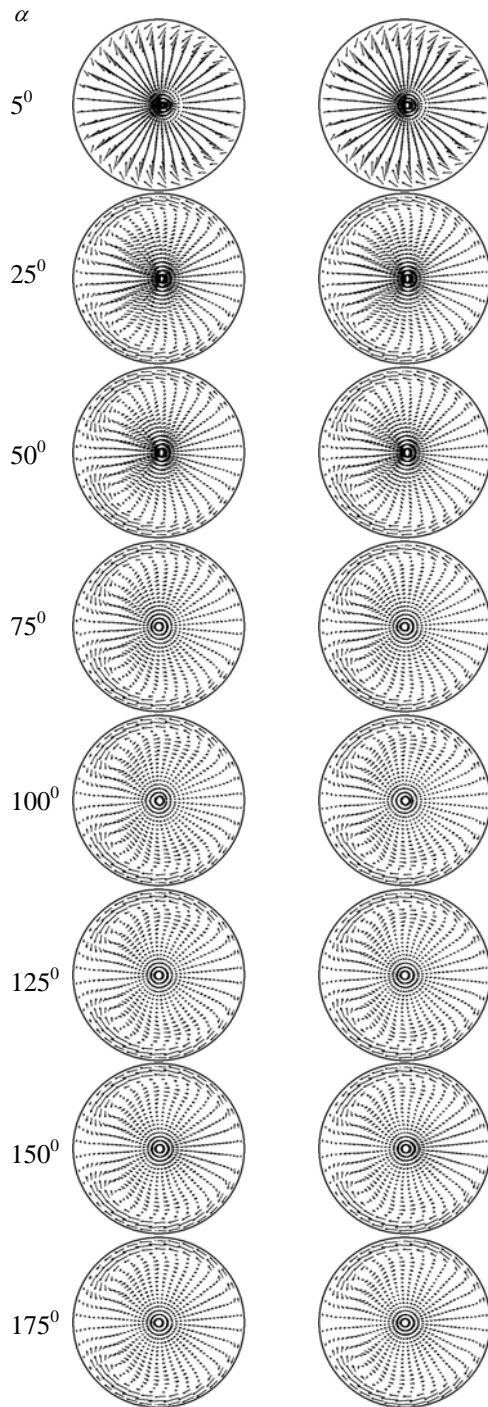
Fig. 4: Vector plots of the secondary flow for $R_e = 900$ and 1100 at curvature $\delta = 0.1$.

Fig. 5: Contour plots of the axial velocity for $R_e = 900$ and 1100 at curvature $\delta = 0.1$.

near the centre of the cross-section increase in the direction of the centrifugal force and the flow in the core region moves radially outward along the horizontal plane passing through the centre of the cross-section. At the same time, the particles near the upper and lower boundary experience high circumferential velocity in the direction opposite to the velocity of the particles at the core region. As a result, two vortex secondary flow is set up. The secondary velocity of the particles in the inner half is higher than the velocity of the particles at the centre and outer half of the cross-section. As a result, two vortices are set up in the inner half.
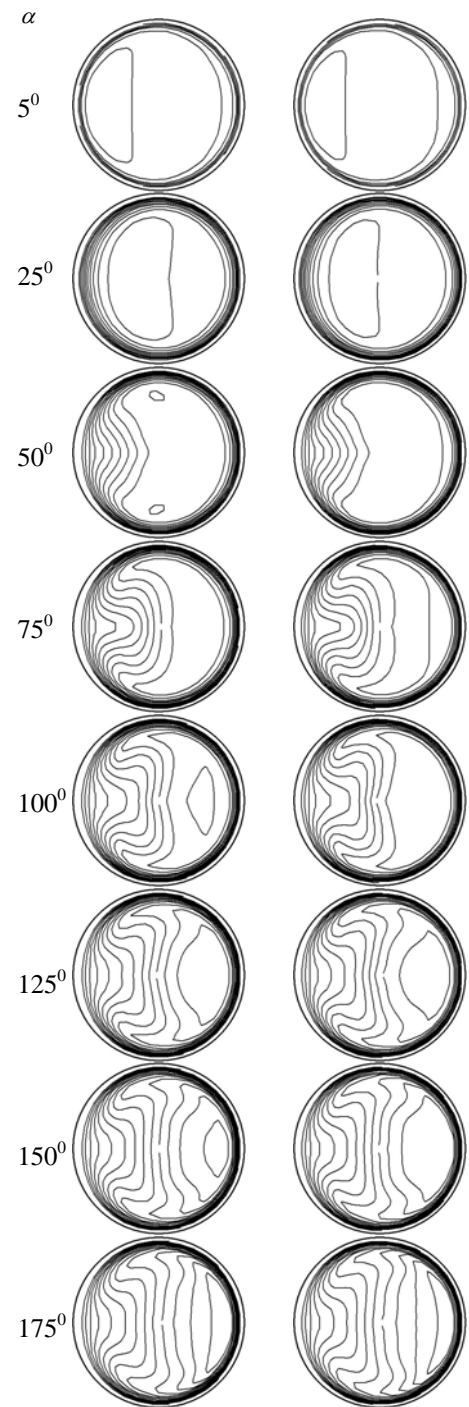
6.2 Axial flow development

The contour plots of the axial velocity has been shown in Fig. 5 for Reynolds number 900 and 1100 respectively. The axial velocity profile of the particles on the horizontal plane passing through the center of cross-section have been shown in Figs. 6, 7. The axial flow is symmetric about the plane passing through the centre of cross-section. As the flow enters the pipe boundary layer begins to develop. Boundary layer near the inner wall develops faster than that at the outer wall. Just after the entrance, the axial velocity of the particles is higher
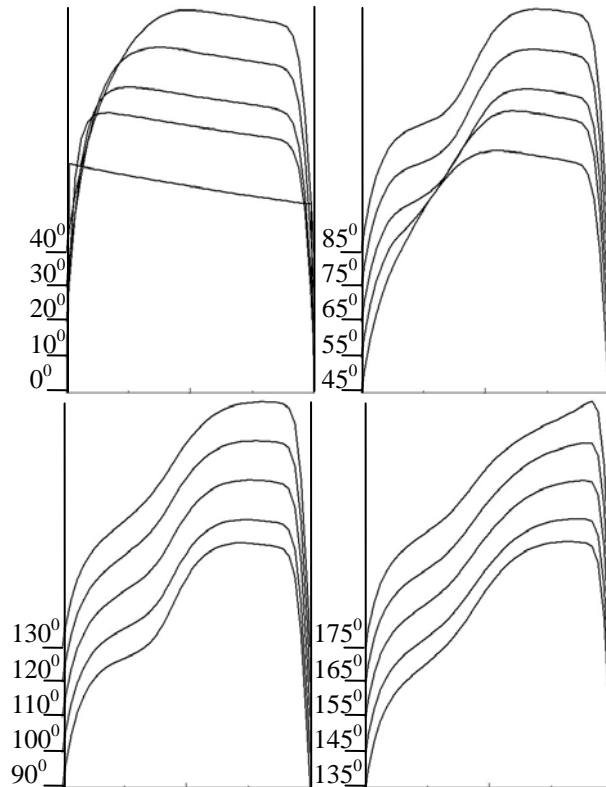
Fig. 6: Axial Velocity profile on the horizontal plane passing through the center of cross-section for $R_e = 900, \delta = 0.10$.
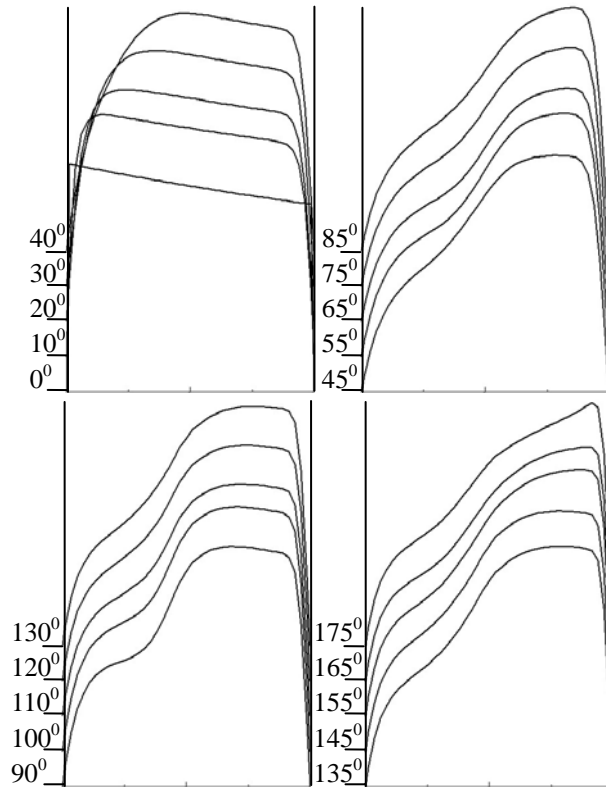

Fig. 7: Axial Velocity profile on the horizontal plane passing through the center of cross-section for $R_e = 1100, \delta = 0.10$.

in the inner half. But as the flow proceed downstream the particles in outer half attains higher velocity. Two step plateau like velocity profile is found at the middle of the pipe. But finally single picked axial velocity is found.

7. REFERENCES

[1] P. C. Sinha and M. Aggarwal, "Entry Flow In A Straight Circular Pipe", Austral. Math. Soc. (Series B), vol. 24, pp. 59-66, 1982.

[2] M. Van Dyke, "Entry flow in a channel", *J. Fluid Mech.*, vol. 44, pp. 813-823, 1970.

[3] W. R. Briley, *Proceedings of 3rd International Conference Numerical Methods in Fluid Dynamics, Paris*, pp. 33-38, 1972.

[4] H. Morihara, and T. S. Cheng, (1973), *Journal of Computational Physics*, 11, pp. 550.

[5] M. P. Singh, "Entry flow in a curved pipe, Journal of Fluid Mechanics", vol. 65, pp. 517-539, 1974, doi:10.1017/S0022112074001522.

[6] M. P. Singh, P. C. Sinha and M. Aggarwal, "Flow in the entrance of the aorta, Journal of Fluid Mechanics", vol. 87, pp. 97-120, 1978, doi:10.1017/S0022112078002955.

[7] W. Y. Soh and S. A. Berger, "Laminar entrance flow in a curved pipe", *Journal of Fluid Mechanics*, vol. 148, pp. 109-135, 1984

[8] M. A. Masud and Md. M. Alam, "Effect of Curvature on Entry Flow", *Proceedings of MARTEC 2010, The International Conference on Marine Technology11-12 December 2010, BUET, Dhaka, Bangladesh*.

8. NOMENCLATURE

Symbol	Meaning
u, v, w	Dimensionless velocity components along radial, circumferential and axial direction respectively
R_e	Reynold's Number
T_r	Taylor Number
δ	Dimensionless curvature